Prediction of Tin-Whiskers Generation Using Stress and Mass-Diffusion Analysis

Takeshi Terasaki

Hitachi, Ltd., Hitachi Research Laboratory

Abstract: *A spreading environmental awareness has prompted a global movement towards lead-free electronic products, in which lead-free tin plating is included. Lead-free tin plating provides good solderability equal to tin-lead plating, however the spontaneous whisker growth on lead-free tin plating is a serious reliability issue. It's imperative to clarify the whisker generation and growth mechanism. So we have developed a multi-scale simulation technique for calculating tin atom diffusion caused by stress gradient induced by temperature change and crystal orientation distribution in polycrystalline tin plating. This multi-scale simulation technique uses molecular dynamics (MD) simulation and a finite element analysis (FEA). The FEA simulates macro-scale stress and stress-induced mass-diffusion, and the MD simulates nano-scale atomic diffusion. The stress analysis model considers elasticity anisotropy, thermal-expansion anisotropy, and the crystal orientation of tin. A thermal cycling test was conducted to induce whisker generation on tin-plated specimens, and the crystalline orientations around the whiskers were evaluated using electron back-scattering diffraction pattern (EBSP) measurement. The hydrostatic pressure distribution and tin-atomic-density distribution in the specimens were calculated using our technique. The whisker locations corresponded to the areas of higher tin-atomic density and lower hydrostatic pressure on the tin-plated surface, indicating that our technique can predict whiskers generation in tin platings.*

Keywords: *Tin whisker, Tin plating, Electronic product, Lead-free, Finite element analysis, Atomic diffusion, Stress gradient, Crystal orientation, Elasticity anisotropy*

1. Introduction

Electronic systems, which include the electronic components, form the foundation for today's convenient and comfortable world. Tin–lead plating is commonly used for electronic components because it has excellent solderability and tin whisker resistance. Tin whiskers are microscopic single-crystal metal fibers which grow from tin platings. They can grow at random and create conductive paths between unintended leads on electronic components. The electrical short-circuits may seriously interfere with performance of electronic systems. However, increasing environmental awareness is leading to restrictions on the use of lead in electronic products worldwide. Many producers are thus using pure tin or tin alloy plating (hereinafter collectively referred to simply as “tin plating”) instead of conventional tin–lead plating because it has the same solderability as tin–lead plating although it is more susceptible to tin whisker generation and growth.

The major factor in the whisker growth is apparently compressive stress generated in the tin plating. This compressive stress induces diffusion and local concentrations of tin atoms, which lead to generation and growth of tin whiskers. Sources of this compressive stress include formation of inter-metallic compounds at the tin/lead-frame interface (Lee, 1998), oxidation of tin (Barsoum, 2004), and cyclical changes in temperature (Zhao, 2006). The three-dimensional finite element analysis (FEA) model established by Zhao et al.—which considers elasticity anisotropy, thermal-expansion anisotropy, and β-tin plasticity—is an effective method for evaluating whisker growth caused by cyclical changes in temperature (Zhao, 2006). However, it does not provide information about the relationship between the strain-energy density and tin-atomic localization induced by atomic diffusion. Tin-atomic localization, that is, the change in the atomic density distribution of the tin, is a key factor in tin whisker growth.

A simulation technique for evaluating the atomic density distribution of tin was developed by our group (Terasaki, 2009). It uses molecular dynamics (MD) simulation for nano-scale atomic diffusion analysis, FEA for macro-scale stress and mass-diffusion analysis, and x-ray diffraction (XRD) for crystalline orientation measurement. We investigated the possible use of this technique to predict the locations of generated whiskers (Terasaki, 2012). Thermal cycling tests were performed to induce whisker generation on tin-plated specimens. The crystalline orientations of the tin film were evaluated in the vicinity of the whiskers using electron back-scattering diffraction pattern (EBSP) measurement. The simulation results indicated that the areas of higher tin-atomic density and lower hydrostatic pressure on the tin-plated surface were consistent with the locations of generated whiskers.

2. Test procedure

2.1 Thermal cycling test

Test pieces were fabricated from a lead frame constructed of 125-μm-thick commercial copper material plated with pure tin to a thickness of 10 μm. The crystal grains in the tin plating were β-tin. After plating, the test pieces were kept at 150°C for one hour, and then a thermal cycling test was conducted. The conditions for the test were −40°C to 85°C, 60 minutes per cycle (20 minutes of holding at low temperature, 10 minutes of heating, 20 minutes of holding at high temperature, and 10 minutes of cooling). There were 1000 cycles.

2.2 Crystal orientation measurement

After the thermal cycle test, we examined the surface of the tin plating with a scanning electron microscope (SEM) and selected a 100 μm × 100 μm region containing multiple whiskers to measure the crystal orientations of the tin grains. Because the tin-plated surface after the thermal cycle test had protrusions and depressions, we shaved 6 μm off the surface of the plating in the horizontal direction using a rotating microtome to enable evaluation of the crystal orientations in the target region by EBSP measurement. We used a TSL MSC-2200 orientation-imaging microscopy system operating at an acceleration voltage of 20 kV for the EBSP measurement. EBSP measurements gave the identified crystal orientations as Bunge Euler angles.

3. Calculation procedure

3.1 Finite element analysis model

For the macro-scale stress and mass-diffusion analysis, we used ABAQUS/Standard version 6.9. An in-house general preprocessor was used to build the FEA model shown in Figure 1. Since the crystal grains in the tin plating had a columnar organization that was as thick as the plating, the grains were modeled as columnar crystals. Their shape was derived from the EBSP measurements. The entire analysis model was constructed in an orthogonal coordinate system (x-y-z), with the tin plating surface in the x-y plane and the plating thickness in the z direction. The analysis region was 102 μm × 105 μm. A 0.1-μm-wide region was set at the crystal grain boundaries. The thickness of the copper lead fame was 100 μm, which is close to the actual thickness. The element segmentation was done using 3D cubic elements with eight nodes (C3D8) to evaluate volume fractions of relative tin atomic density at grain boundaries (Terasaki, 2009), resulting in an analysis scale of 219,472 nodes and 206,130 elements.

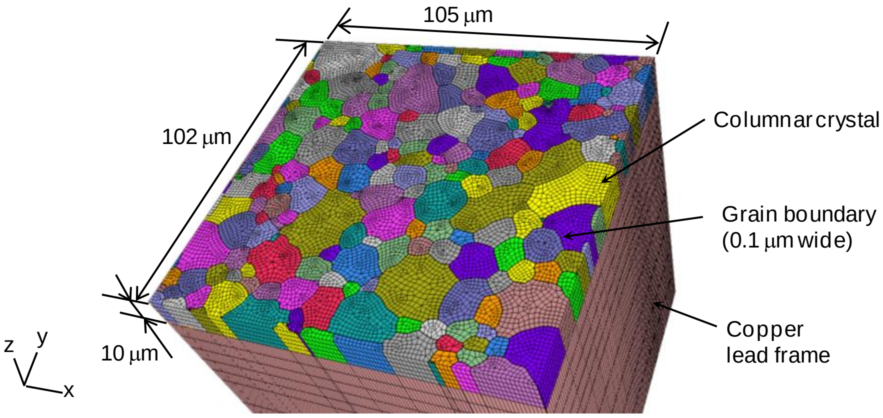

Figure 1. FEA model for stress and mass-diffusion analysis.

3.2 Macro-scale stress analysis

The crystals in the tin plating are β-tin. Since β-tin has an orthotropic body-centered tetragonal structure with *c*-axis about half the length of its *a*-axis, orthotropic elasticity and thermal expansion orthotropy are significant (Revelo, 1997). The elastic constants of β-tin are listed in Table 1 (Allard, 1969), where 1, 2, and 3 indicate the perpendicular components of the *a*, *b*, and *c* axis directions and 4, 5, and 6 indicate the respective cross-section components for the 12, 23, and 31 directions. The coefficient of thermal expansion (CTE) of β-tin is $\alpha_1 = \alpha_2 =$ 15.8×10^{-6} /°C, and $\alpha_3 =$ 28.4×10^{-6} /°C (Zhao, 2006). A local orthogonal coordinate system (1-2-3) was defined for each column-modeled crystal, and the Euler angle determined by EBSP measurement was set as the angle of rotation of the local orthogonal coordinate system relative to the overall orthogonal coordinate system.

The copper lead frame was assumed to be an isotropic elastic body with a Young's modulus of 127 GPa, a Poisson ratio of 0.3, and a CTE of 17.0×10^{-6} /°C. Since the macro CTE of the tin plating was higher than that of the copper lead frame, an increase in temperature created compressive stress in the tin plating. As mentioned above, this compressive stress is apparently the major factor in whisker growth. Accordingly, we subjected the FEA model to a thermal load produced by a uniform 100°C (i.e., 25°C to 125°C) rise in temperature.

Symmetric boundary conditions were applied to two cross sections of the 3D model (the lower left area in Figure 1). Two other cross sections (the upper right area in Figure 1) were modeled under a node-coupling boundary condition. The tin-plated surface was modeled under a free-boundary condition. The bottom of the lead frame was fixed in the z direction.

Table 1. Material constants of tin crystal.

Elastic tensor component	C_{11}, C_{22}	C_{33}	C_{44}, C_{55}	C_{66}	C_{12}	C_{13},C_{23}
Material constant (GPa)	72.30	88.40	22.03	24.00	59.40	35.78

3.3 Macro-scale diffusion analysis

Abaqus/Standard provides the general mass-diffusion analysis capabilities. The governing equations for mass-diffusion are an extension of Fick's equations, which allow for mass diffusion driven by gradients of temperature and pressure (Abaqus Users Manual):

$$\mathbf{J} = -s\mathbf{D}\cdot\left[\frac{\partial\phi}{\partial\mathbf{x}} + \kappa_s\frac{\partial\left(\ln\left(\theta-\theta^z\right)\right)}{\partial\mathbf{x}} + \kappa_p\frac{\partial p}{\partial\mathbf{x}}\right], \tag{1}$$

where $\mathbf{J}$ is concentration flux in the diffusing phase; s is solubility; ϕ is the “normalized concentration, i.e., $\phi = c/s$, where c is the mass concentration; $\mathbf{D}(c,\theta,\boldsymbol{f})$ is diffusivity; $\kappa_s(c,\theta,\boldsymbol{f})$ is the “Soret effect” factor (diffusion driven by temperature gradient); θ is temperature; θ^z is absolute zero on the temperature scale used; $\kappa_p(c,\theta,\boldsymbol{f})$ is the pressure stress factor (diffusion driven by gradient of equivalent pressure stress p); and $\boldsymbol{f}$ is any predefined field variable. The boldface letters represent tensors.

In general, atoms diffuse at grain boundaries because the coefficient of grain-boundary diffusion is much higher than the coefficient of intra-particle diffusion. The stress-induced atomic flow along a grain boundary, J_α , is defined as a function of the stress perpendicular to the grain boundary, σ_v (Needleman, 1980):

$$J_\alpha(x_\alpha) = -\frac{D_\alpha}{\kappa T}\frac{\partial\mu}{\partial x_\alpha}, \tag{2}$$

$$\mu = \mu_0 - \sigma_v \Omega, \tag{3}$$

where D_α is the coefficient of grain-boundary diffusion, κ is Boltzmann's constant, T is absolute temperature, x_α is a local coordinate system along the grain boundary, μ is the chemical potential, μ_0 is the reference potential, and Ω is atomic volume. Assuming a proportional relationship between the stress perpendicular to the grain boundary, σ_v, and hydrostatic pressure p makes it possible to use the mass-diffusion analysis function of the ABAQUS/Standard software for grain-boundary diffusion analysis. Hydrostatic pressure is written as

$$p = -trace(\boldsymbol{\sigma})/3, \tag{4}$$

where $\boldsymbol{\sigma}$ is a stress tensor.

Mass-diffusion analysis based on Equation 1 was conducted using the FEA models shown in Figure 1. The values of p were obtained from the stress analysis described in the previous section. Steady-state analysis was performed because the holding time used in the thermal-cycling test (20 minutes) was sufficient for stabilizing the diffusion behavior of tin atoms. The initial concentration was 100 %, and the solubility was 1. Since a uniform thermal load was used in the modeling, the temperature gradient effect was ignored, i.e., $\kappa_s = 0$.

3.4 Nano-scale atomic diffusion analysis

To conduct mass-diffusion analysis by FEA, we needed the value of diffusion coefficient D for solid-state β-tin. Since this value has not been reported, we estimated the values of the self-diffusion coefficient and grain-boundary diffusion coefficient of β-tin by MD simulation. To simplify the mass-diffusion analysis, D was assumed to be isotropic.

The number of atoms in the bulk model was assumed to be 1×10^4, and that in the grain-boundary model was assumed to be 2×10^4. To take into account the diffusion of copper atoms from the copper lead frame, we assumed tin with 1 atomic percent of copper as the bulk model. The boundary between grain A and grain B was assumed to be $\Sigma\,5(110)$. Periodic boundary conditions were applied in the x, y, and z directions in each model. To take into account the dependence of stress on the diffusion coefficient, we calculated the diffusion coefficients at 20°C under compressive stress σ_x normal to the grain boundary acting on the system at 0, 50, and 200 MPa.

4. Test results

4.1 Whisker growth locations

An SEM photograph of a tin-plated surface after the thermal cycle test is shown in Figure 2. The protrusions and depressions correspond to tin columnar crystals. We consider the protrusions to be very short whiskers. Five very short whiskers are evident in the 102 μm × 105 μm region. The whisker locations are indicated by yellow arrows. Five depressed areas, indicated by pink arrows, are evident near the whiskers. From the adjacency of the whiskers and the depressions, we can infer that tin atoms from the depressions fed the growth of the whiskers.

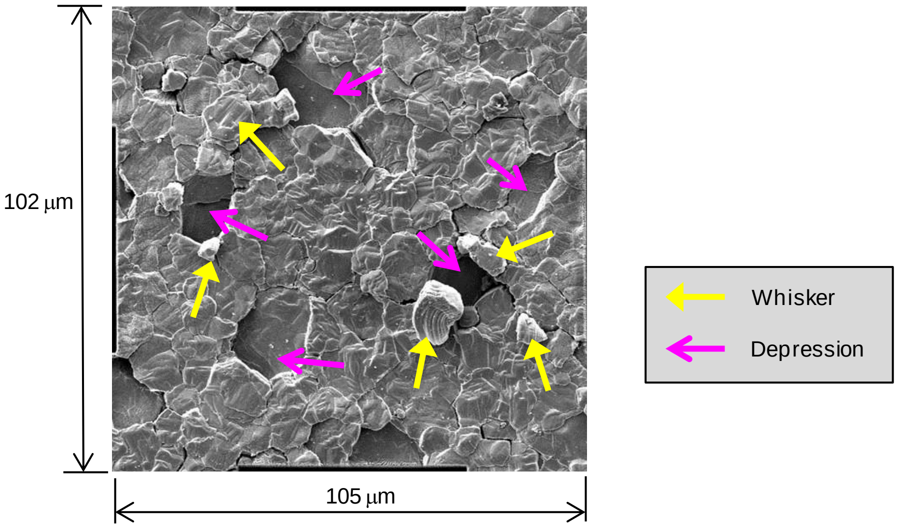

Figure 2. SEM image of tin-plated surface after thermal cycling test.

4.2 Crystal orientation measurement

The crystal orientations within the tin plating shown in Figure 2 were evaluated by shaving a 6-μm layer off the surface of the plating and then performing EBSP measurement, as mentioned above. The shapes and crystal orientations of the measured crystal grains are shown in Figure 3. There were 215 crystal grains within the measured area. The whisker growth areas (enclosed by light yellow lines in the figure) include many pink-colored crystal grains, which have an orientation close to (001). The depressed regions enclosed by the pink lines include blue or green grains, which respectively have orientations of close to (110) or (100). We performed a stress analysis that took crystal orientation into account.

As previously mentioned, β-tin has a large CTE in the *c*-axis direction. The CTE of the (001)-oriented crystal grains in the planar direction of the tin plating was about the same as that of the copper lead frame because the *c*-axis of the crystal grains is in the depth direction of the tin plating. Therefore, a temperature change produced very little stress in the tin plating. The *c*-axes of the (110)- and (100)-oriented crystals, however, were in the plane of the tin plating. Therefore, the CTE of the grains was greatly different than that of the copper lead frame, and a change in temperature produced large stress in the tin plating.

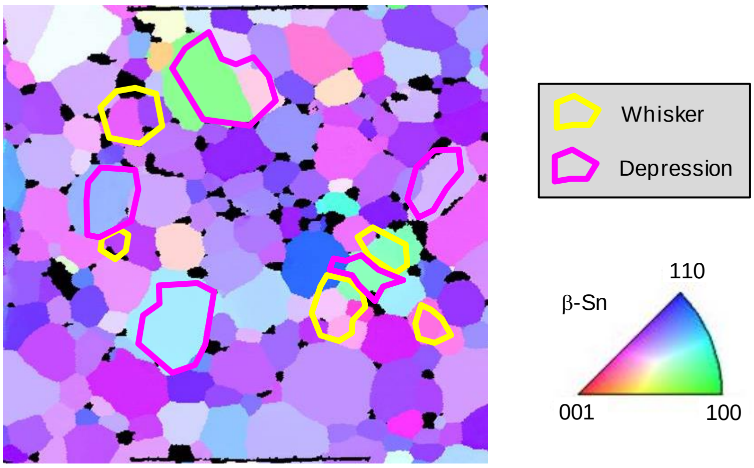

Figure 3. Shapes and crystal orientations of measured crystal grains.

5. Calculation results

5.1 Diffusion coefficients

The diffusion coefficients estimated by MD simulation are illustrated in Figure 4. The diffusion coefficients at the grain boundaries were much higher than those in the grains, indicating that compressive stress increases the diffusion coefficient. Although it is believed that grain-boundary diffusion is a more dominant factor in tin whisker growth than bulk diffusion, the MD model can quantify the difference between grain-boundary diffusion and bulk diffusion. The simulated diffusion coefficients were used in the following mass-diffusion analysis, and κ_p at 1 was estimated roughly from the MD calculation results.

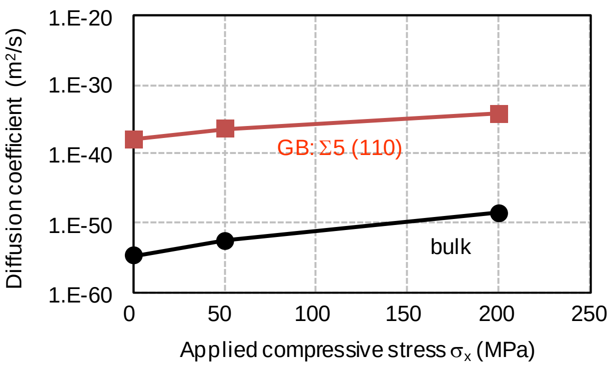

Figure 4. Simulated diffusion coefficients in bulk and at grain boundary.

5.2 Hydrostatic-pressure distribution

Figure 5 plots the hydrostatic pressure distribution on the tin-plated surface obtained from the stress analysis. The orange and red indicate regions in which there was hydrostatic pressure of from 40 to 50 MPa and stronger compressive stress. The light blue and dark blue indicate regions in which there was hydrostatic pressure of from 0 to 15 MPa and weaker compressive stress. The black indicates regions in which there was negative hydrostatic pressure and tensile stress of near zero. The whisker growth locations and depressed areas indicated by the arrows in Figure 2 are respectively marked by light yellow and pink polygons in Figure 5.

The whisker locations are consistent with regions where the hydrostatic pressure was 10 MPa or less. The depressed areas are, with one exception, regions of from 20 to 30 MPa hydrostatic pressure that lie between regions of weak hydrostatic pressure of 10 MPa or less. Because whisker growth results from atomic diffusion driven by compressive stress, the crystal grains in the depressed areas supply the atoms required for whisker growth. It is thus clear that stress analysis that takes into account the anisotropy of elasticity and CTE of the tin-crystal grains and the crystal shape can be used to predict the locations of whiskers that grow during a thermal cycle test.

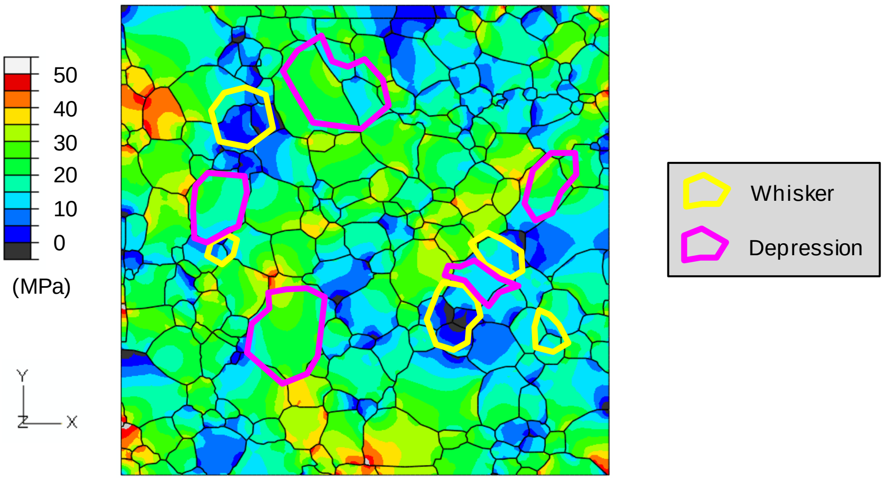

Figure 5. Hydrostatic-pressure distribution on tin-plated surface.

5.3 Tin-atomic-density distribution

Figure 6 plots the tin-atomic-density distribution on the tin-plated surface obtained from the diffusion analysis. Comparing it with the hydrostatic pressure distribution shown in Figure 5, we see that regions of high hydrostatic pressure (30 MPa or more) correspond to the low concentration areas and that regions of low hydrostatic pressures (10 MPa or less) correspond to the high concentration areas.

In Figure 6 the locations of whiskers and depressions are respectively marked with light yellow and pink polygons. At the whisker positions and in their vicinities, there are portions where the tin-atomic density was high, which confirms that tin-atomic diffusion driven by compressive stress is the mechanism for whisker growth. In the depressed areas, the tin-atomic density was not low, but the tin-atomic density in the vicinity of the depressed areas was low. Therefore, we can conclude that regions of high compressive stress near whisker locations supply atoms for whisker growth.

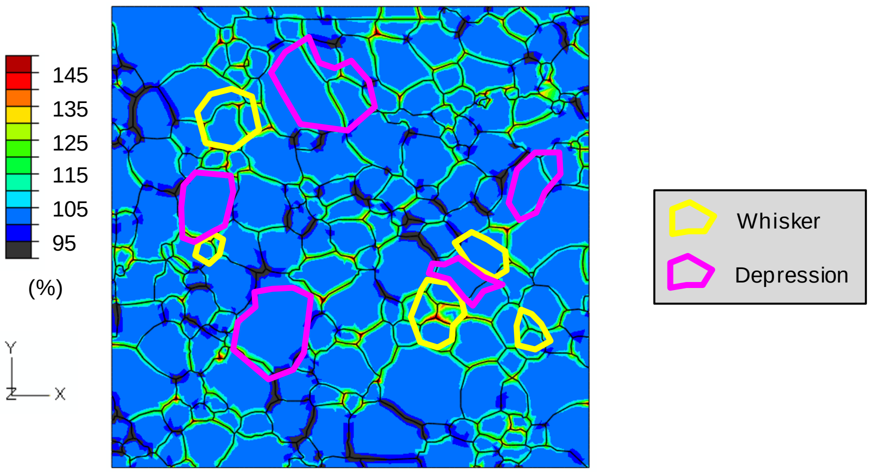

Figure 6. Tin-atomic-density distribution on tin-plated surface.

6. Conclusion

We have shown that a developed simulation technique can be used to predict the locations of whiskers that grow on tin plating during a thermal cycle test. We first fabricated tin plating on a copper lead frame, performed a thermal cycle test, observed the whisker formation, and evaluated the crystal orientations of the crystal grains in the region of whisker growth by EBSP measurement. Next, we used the crystal orientation measurements to perform a stress-diffusion analysis, which showed that the areas of low hydrostatic pressure and high tin-atom density were consistent with the locations of whisker formation.

7. References

1. Allard, S., “International Tables of Selected Constants Vol. 16, Metals”, Thermal and Mechanical Data, Pergamon Press, Oxford , 1969
2. Barsoum, M. W., Hoffman, E. N., Doherty, R. D., Gupta, S. and Zavalaingos, A., “Driving force and mechanism for spontaneous metal whisker formation,” Phys. Rev. Lett., vol. 93, article number 206104, 2004.
3. Lee, B.-Z. and Lee, D. N., “Spontaneous growth mechanism of tin whiskers,” Acta Mater., vol. 46, no. 10, pp. 3701–3714, 1998
4. Needleman , A. and Rice, J.R., Acta Metallurgica, vol. 28, p. 1315, 1980.
5. Ravelo, R. and Baskes, M., “Equilibrium and thermo-dynamic properties of grey, white, and liquid tin,” Phys. Rev. Lett., vol. 79, no. 13, pp. 2482–2485, 1997.
6. Terasaki, T., Iwasaki, T., Ookura, Y., Suzuki, T., Kato, T., Nakamura, M. and Hashimoto, T., “Evaluation of Tin-whisker Growth During Thermal-cycle Testing Using Stress- and Mass-diffusion Analysis”, Proc 59th Electronic Components and Technology Conf, San Diego, CA, pp. 277–284, 2009.
7. Terasaki, T., Kato, T., Iwasaki, T., Ookura, Y., Nakamura, M., Ishii, H. and Yamamoto, K., “Prediction of Tin-Whiskers Generation during Thermal Cycle Test Using Stress and Mass-Diffusion Analysis”, Proc 62nd Electronic Components and Technology Conf, San Diego, CA, pp. 1183 - 1189, 2012.
8. Zhao, J.H., Su, P., Ding, M., Chopin, S. and Ho, P. S., “Microstructure-Based Stress Modeling of Tin Whisker Growth”, IEEE Transactions of Electronics Packaging Manufacturing, vol. 29, no. 4, pp. 265–273, 2006.
9. Abaqus Users Manual, Version 6.9, Dassault Systemns Simulia Corp., Providence, RI.